Chinese Chemical Letters 33 (2022) 3172–3176

Contents lists available at ScienceDirect

Chinese Chemical Letters

journal homepage: www.elsevier.com/locate/cclet

# Activation of peracetic acid by metal-organic frameworks (ZIF-67) for efficient degradation of sulfachloropyridazine

Jun Duan[a,b], Long Chen[a], Haodong Ji[a,b], Peishen Li[a], Fan Li[a,b], Wen Liu[a,b,*]

[a] The Key Laboratory of Water and Sediment Science, Ministry of Education, College of Environment Science and Engineering, Peking University, Beijing 100871, China

[b] State Environmental Protection Key Laboratory of All Material Fluxes in River Ecosystems, Peking University, Beijing 100871, China

ARTICLE INFO

*Article history:*
Received 22 September 2021
Revised 9 November 2021
Accepted 24 November 2021
Available online 29 November 2021

*Keywords:*
Peracetic acid activation
Metal-organic frameworks
Zeolitic imidazole framework (ZIF)-67
Emerging organic contaminants
Acetylperoxy radical
DFT calculation

ABSTRACT

Peracetic acid (PAA)-based system is becoming an emerging advanced oxidation process (AOP) for effective removal of organic contaminants from water. Various approaches have been tested to activate PAA, while no previous researches reported the application of metal-organic frameworks (MOFs) materials for PAA activation. In this study, zeolitic imidazole framework (ZIF)-67, a representative MOFs, was facile synthesized *via* direct-mixing method at room temperature, and tested for PAA activation and sulfachloropyridazine (SCP) degradation. The as-synthesized ZIF-67 exhibited excellent performance for PAA activation and SCP degradation with 100% of SCP degraded within 3 min, owing to the specific MOFs structure and abundant $Co^{2+}$ sites. The *pseudo*-first-order kinetic model was applied to fit the kinetic data, with rate constant $k_1$ of ZIF-67 activated PAA system 34.2 and 156.5 times higher than those of conventional $Co_3O_4$ activated PAA and direct oxidation by PAA. Radical quenching experiments and electron paramagnetic resonance (EPR) analysis indicated that $CH_3C(O)OO^{\bullet}$ played a major role in this PAA activation system. Then, the Fukui index based on density functional theory (DFT) calculation was used to predict the possible reaction sites of SCP for electrophilic attack by $CH_3C(O)OO^{\bullet}$. In addition, the degradation pathway of SCP was proposed based on Fukui index values and intermediates detection, which mainly included the S-N bond cleavage and $SO_2$ extrusion and followed by further oxidation, dechlorination, and hydroxylation. Therefore, ZIF-67 activated PAA is a novel strategy and holds strong potential for the removal of emerging organic contaminants (EOCs) from water.



Advanced oxidation processes (AOPs) have been widely applied in the advanced treatment of organic contaminants in water treatment plants (WTPs) and wastewater treatment plants (WWTPs) [1–4], owing to the generation of strong reactive oxygen species (ROSs). Among the AOPs, *in situ* activations of peroxides is an effective approach to readily generate abundant ROSs, including hydrogen peroxide ($H_2O_2$, HP), peroxymonosulfate ($HSO_5^-$, PMS), and persulfate ($S_2O_8^{2-}$, PS) [5–8]. In recent years, activation of peracetic acid (PAA) has been intensively tested to remove various organic contaminants from water, which involves the generation of hydroxyl radicals ($^{\bullet}OH$) and organic radicals such as acetylperoxy radical ($CH_3C(O)OO^{\bullet}$) and acetoxyl radical ($CH_3C(O)O^{\bullet}$) [9,10]. Compared to HP and PMS, the bond energy of O–O of PAA (159 kJ/mol) was lower than that of HP (213 kJ/mol) and PMS (317 kJ/mol) [9], suggesting the easier activation of PAA. Typically, PAA can be activated by the external energy, such as ultraviolet (UV) irradiation, heat, and ultrasonic (US) irradiation [11–13]. However, the usage of external energy would inevitably increase the operation cost and the complexity of the water treatment unit. Alternatively, homogeneous activation of PAA using transition metal ions ($Co^{2+}$, $Fe^{2+}$, and $Mn^{2+}$) seems a feasible and energy-saving approach since the only input for PAA activation is the metal ion chemicals [10,14–17]. Unfortunately, homogeneous activation has some intrinsic drawbacks that limit its large-scale application. First, it is difficult to recycle the metal ions from the treated water, which requires a continuous chemical input and may need a second treatment to remove the metal ions from water [1]. Second, metal ions are vulnerable to various water chemistry conditions and can form precipitation or complexes with water matrix, thereby hindering the PAA activation efficiency [14]. Instead, heterogeneous activation of PAA by catalysts is a more promising method to overcome the drawbacks of homogeneous system. Previously, metal oxides ($Co_3O_4$, $Fe_2O_3$, and $MnO_2$) have been successfully applied in PAA activa-

* Corresponding author at: The Key Laboratory of Water and Sediment Science, Ministry of Education, College of Environment Science and Engineering, Peking University, Beijing 100871, China.
*E-mail address:* wen.liu@pku.edu.cn (W. Liu).

https://doi.org/10.1016/j.cclet.2021.11.072
1001-8417/

tion [12,18]. Nevertheless, the metal oxides catalysts still show limited specific surface area, pore volume and structure, and reactive sites for PAA activation. Recently, metal-organic frameworks (MOFs), with metal ions as nodes and organic ligands as linkage, have been largely studied in PMS and PS activation, owing to their large specific surface area (SSA), tunable pore structure, and abundant reactive sites [19–21]. To the best of our limited knowledge, there has been no previous researches that studied the activation of PAA by any MOFs materials, which holds the strong potential as a novel strategy to remarkably enhance the PAA activation efficiency. Herein, a representative cobalt-based MOFs, zeolitic imidazole framework (ZIF)-67 were first time employed to activate PAA, which is due to the excellent activation performance of cobalt for PAA and facile preparation of ZIF-67 under ambient conditions [14,22]. In addition, sulfachloropyridazine (SCP), a widely used broad-spectrum sulfonamide antibiotic for bacterial infections in animals [23,24], was chosen as the probe contaminant in this study, since trace amount of SCP in water may cause ecotoxicity and antibiotic resistance genes (ARGs) to aquatic organisms and finally impact the human health [25]. The overall goal of this study was to explore the performance of PAA activation by ZIF-67 and the degradation of SCP. Specifically, the detailed objectives were to: (1) synthesize and characterize ZIF-67 using various characterization approaches; (2) examine the PAA activation and SCP degradation by ZIF-67 *via* batch kinetics tests; (3) elucidate the detailed mechanism of PAA activation and SCP degradation through experimental detection and density functional theory (DFT) calculation.

All chemicals were of analytical or higher grade and were used without further purification. The salient properties of SCP were listed in Table S1 (Supporting information). Ultrapure water (18.2 MΩ·cm) was used in this study to prepare the chemical stock solution (SS) and working solution (WS). Detailed information on chemicals was provided in Text S1 (Supporting information).

ZIF-67 was synthesized following a facile method with the modified recipe by mixing cobalt nitrate hexahydrate ($Co(NO_3)_2 \cdot 6H_2O$) and 2-methylimidazole using methanol as solvent at room temperature [22,26,27]. Briefly, 1.455 g of $Co(NO_3)_2 \cdot 6H_2O$ and 2.463 g of 2-methylimidazole were separately transferred into 100 mL of methanol in a beaker and sonicated for 5 min and stirred for 30 min to completely dissolve the chemicals. Then, $Co(NO_3)_2 \cdot 6H_2O$ solution was dropwise added into 2-methylimidazole solution under vigorous stirring and mixed for 24 h. Afterward, the purple precipitate was collected by filtration, washed with methanol three times, and dried in the oven at 65 °C for 24 h. Fig. S1 (Supporting information) presented the molecular structure of ZIF-67. For comparison, commercial $Co_3O_4$ was purchased from Macklin Biochemical Co., Ltd. (Shanghai, China) and used in this study for PAA activation and SCP degradation.

The as-prepared material was characterized through field-emission scanning electron microscope (FESEM), powder X-ray diffraction (XRD), X-ray photoelectron spectroscopy (XPS), Fourier-transform infrared (FTIR) spectrometer, and zeta potential ($\zeta$). Details of characterization were given in Text S2 (Supporting information).

Catalytic activation of PAA and degradation of SCP were conducted in 100 mL of amber glass batch reactors at room temperature. Specifically, the initial concentration of SCP and PAA was set as 10 and 50 μmol/L, respectively, and the solution pH was adjusted to 7.0 ± 0.2 using 0.1 mol/L of NaOH and $H_2SO_4$. Then, the catalytic reaction was initiated by transferring 50 mg of ZIF-67 into the 100 mL solution (ZIF-67 dosage = 0.05 g/L) under magnetic stirring at 500 rpm. After a predetermined time interval, 1 mL of suspension was sampled and immediately filtered through a 0.22 μm syringe filter (nylon) and quenched with 2 mmol/L of $Na_2S_2O_3$ solution. The residual concentration of SCP was analyzed by Agilent 1260 Infinity high-performance liquid chromatography (HPLC, Agilent, USA). In addition, the degradation intermediates of SCP were analyzed by Dionex UltiMate 3000 Series (Thermal Fisher Scientific, USA) ultra-high-performance liquid chromatography (UHPLC) equipped with Q-Exactive Plus Orbitrap mass spectrometer (Q-Exactive Orbitrap MS, Thermal Fisher Scientific, USA). Analytical details were given in Text S3 (Supporting information).

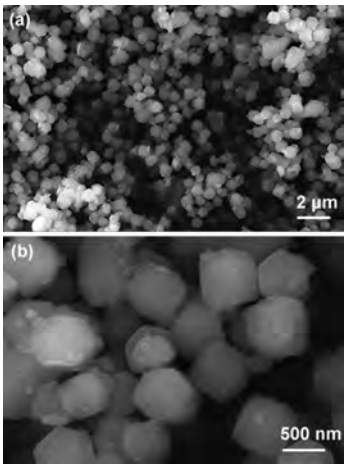


**Fig. 1.** FE-SEM images of ZIF-67 with different magnification. (a) low-magnification; (b) high-magnification.

To explore the active species of PAA activation by ZIF-67, batch tests were conducted by adding 10 mmol/L of *tert*-butyl alcohol (TBA) and ethanol to quench $^{\bullet}OH$ radicals and all radicals, respectively [9,28]. Moreover, the electron paramagnetic resonance (EPR) technique was employed using 5,5-dimethyl-1-pyrroline-*N*-oxide (DMPO) as a trapping agent to directly detect the ROSs formed in this process. Details of EPR analysis were described in Text S4 (Supporting information).

Moreover, the reactive sites of SCP for ROSs attacking were estimated using Fukui index based on DFT calculation to gain insight into the reaction mechanism, which was carried on Gaussian 16 C.01 software [29] and details of calculation were documented in Test S5 (Supporting information).

Fig. 1 presents the SEM images of as-prepared ZIF-67 with different magnification. ZIF-67 shows uniform rhombic dodecahedron morphology (Fig. 1a), which is consistent with previous literature [26,30]. In the close-up observation (Fig. 1b), the ZIF-67 particles have a diameter of *ca*. 600 nm.

The crystallinity of the materials was examined by XRD (Fig. 2a). The sharp peaks of ZIF-67 indicate the good crystallinity of the material. The major peaks at 7.4°, 10.4°, 12.7°, 14.7°, 16.4°, 18.0°, 22.1°, 24.5°, 26.7°, 29.6°, 30.5°, 31.5°, 32.4° were well indexed to (011), (002), (112), (022), (013), (222), (114), (233), (134), (044), (334), (244) and (235) planes of ZIF-67 (CCDC: 671073), respectively, which was in good agreement with previous results [30–32]. In addition, the XRD pattern of $Co_3O_4$ used for comparison matched with the result reported in other literature. Specifically, sharp peaks at 19.1°, 31.3°, 36.9°, 44.9°, 55.7°, 59.4° and 65.3° were assigned to (111), (220), (311), (400), (422), (511) and (440) planes of $Co_3O_4$ (JCPDS #43–1003), respectively [18,33].

XPS study was conducted to gain the elemental composition and coordination information of ZIF-67. In survey XPS spectra of ZIF-67 (Fig. 2b), elements C, N, O, and Co were observed, which agrees with the chemical formula of ZIF-67. Deconvolution of high-resolution XPS spectra of N 1s (Fig. 2c) shows two peaks centered at 398.8 and 395.5 eV, which were ascribed to pyridinic N coordinated with Co and C–N, respectively [22,34]. In the high-resolution spectra of Co 2p (Fig. 2d), two major peaks at 781.2 (Co $2p_{3/2}$) and 796.8 eV (Co $2p_{1/2}$) were in good agreement with Co(II) [22,35].

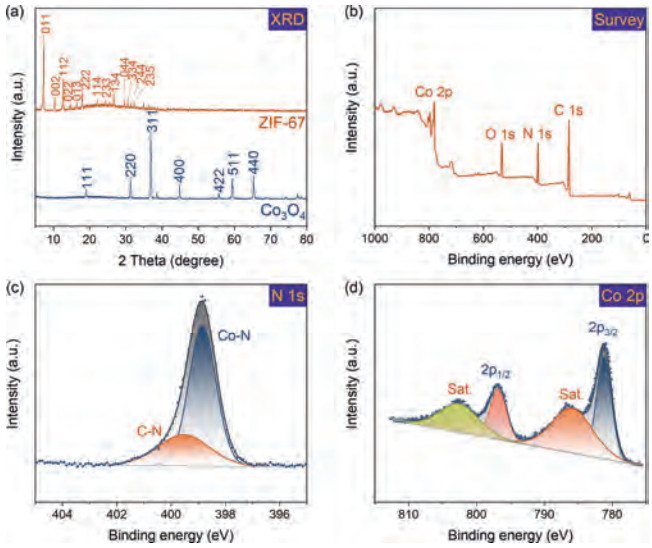


**Fig. 2.** (a) PXRD patterns of ZIF-67 and $Co_3O_4$, ZIF-67; (b) Survey XPS spectra of ZIF-67; (c, d) high-resolution XPS spectra of and N 1s and Co 2p.

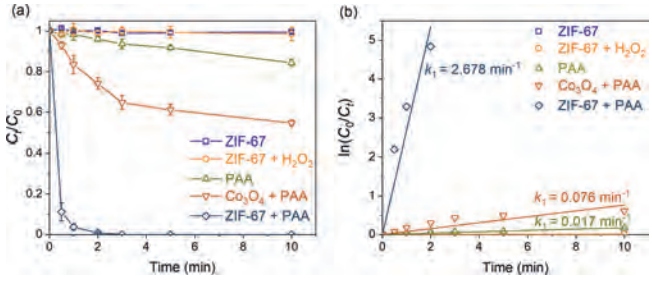


**Fig. 3.** (a) Catalytic degradation of SCP in various systems; (b) *pseudo* first-order model fitting of the kinetic tests. Experimental conditions: [SCP] = 10 μmol/L, [PAA] = 50 μmol/L, [$H_2O_2$] = 250 μmol/L, [catalysts dosage] = 0.05 g/L, pH = 7.0 ± 0.2, and temperature = 25 ± 1 °C.

The two small peaks at 785.9 and 802.5 eV were characteristic shakeup satellite peaks of Co(II) [22,35].

FTIR was further examined to elucidate the coordination information of ZIF-67 and several sharp peaks were observed in FTIR spectra (Fig. S2 in Supporting information). The bands between 500 and 800 cm$^{-1}$, 900–1350cm$^{-1}$, and 1350–1500 cm$^{-1}$ could be assigned to out-of-plane bending vibration, in-plane bending vibration, and stretching vibration of imidazole ring, respectively [22,36]. Two minor peaks at 1379 and 1456 cm$^{-1}$ were attributed symmetric and asymmetric stretching vibration of methyl groups of 2-methylimidazole [36]. Besides, the peak at 1573 cm$^{-1}$ was attributed to the stretching vibration of C=N of 2-methylimidazole [22]. More importantly, a strong peak at 424 cm$^{-1}$ was due to the Co-N stretch mode, suggesting the coordination between $Co^{2+}$ and 2-methylimidazole in ZIF-67. Again, the FTIR result provided evidence of the successful preparation of ZIF-67.

Combining the results of SEM, XRD, XPS, and FTIR, the as-synthesized ZIF-67 showed uniform rhombic dodecahedron morphology with $Co^{2+}$ coordinated with 2-methylimidazole to form MOFs structure. The uniform MOFs structure and abundant exposed Co sites would benefit the follow-on PAA activation and SCP degradation.

Batch kinetic tests were then conducted to evaluate the performance of ZIF-67 for PAA activation and SCP degradation (Fig. 3), and the kinetic data were fitted with the *pseudo*-first-order kinetic model (Eq. 1) [37,38]. ZIF-67 showed no adsorption for SCP within

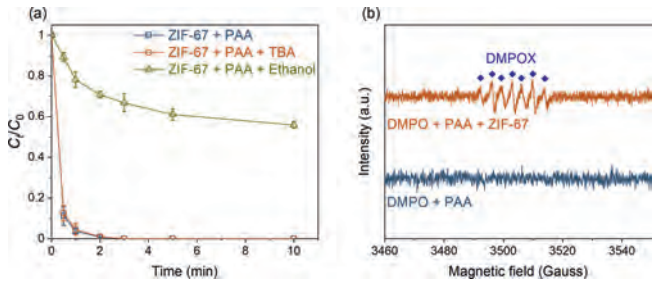


**Fig. 4.** (a) Effects of TBA and ethanol on SCP degradation in ZIF-67 activated PAA system. Experimental conditions: [SCP] = 10 μmol/L, [PAA] = 50 μmol/L, [scavengers] = 10 mmol/L, [catalysts dosage] = 0.05 g/L, pH = 7.0 ± 0.2, and temperature = 25 ± 1 °C; (b) EPR spectra in various systems. Experimental conditions: [DMPO] = 100 mmol/L, [PAA] = 50 μmol/L, [catalysts dosage] = 0.05 g/L.

10 min. SCP was in anionic form at pH 7 (Fig. S3 in Supporting information), while ZIF-67 carried positive charge at pH 7 (Fig. S4 in Supporting information). The low adsorption capacity of ZIF-67 for SCP may due to the lack of appropriate adsorption sites, which was consistent with the previous research [39]. ZIF-67 could not activate $H_2O_2$ to generate ROSs to degrade SCP, which was consistent with the previous finding that $Co^{2+}$ was not able to activate $H_2O_2$ [14]. 15.6% of SCP was removed in the presence of 50 μmol/L PAA, with *pseudo*-first-order rate constant ($k_1$) of 0.017 min$^{-1}$ (Table S2 in Supporting information), showing the strong oxidation ability of PAA. In the $Co_3O_4$ activated PAA system, 45.3% of SCP was degraded with a $k_1$ value of 0.076 min$^{-1}$, showing the good activation performance of $Co_3O_4$ for PAA [18]. In comparison, ZIF-67 showed a dramatic activation effect for PAA, since 100% of SCP was degraded within 3 min and $k_1$ value reached 2.678 min$^{-1}$ (Table S2), which was 34.2 and 156.5 times higher than those of $Co_3O_4$ activated PAA and direct oxidation by PAA, respective. The remarkably enhanced PAA activation was likely due to the MOFs structure of ZIF-67 with large specific surface area and abundant available $Co^{2+}$ sites, while commercial $Co_3O_4$ has limited surface sites.

$$\ln(C_0/C_t) = k_1 \cdot t \quad (1)$$

where $C_0$ and $C_t$ were concentrations of SCP at initial and at time $t$ (min) in water, respectively, while $k_1$ is the rate constant of the *pseudo*-first-order kinetic model (min$^{-1}$).

To explore the major ROSs in the ZIF-67 activated PAA system that contributed to the SCP degradation, radicals quenching experiments were first conducted by using TBA and ethanol as $^{\bullet}OH$ radical scavenger ($k_{TBA/^{\bullet}OH}$ = 3.8–7.6 × 10$^8$ L mol$^{-1}$ s$^{-1}$) and all radicals scavenger, respectively Fig. 4a) [1,11]. In the presence of 10 mmol/L of TBA, no significant decrease of SCP removal efficiency was observed, indicating $^{\bullet}OH$ played little or no role in SCP degradation, which was in agreement with the previous finding that $^{\bullet}OH$ was not the major radical in $Co^{2+}$ activated PAA [9]. Ethanol is also a common scavenger to quench various radicals including $^{\bullet}OH$ ($k_{ethanol/^{\bullet}OH}$ = 1.2–2.8 × 10$^9$ L mol$^{-1}$ s$^{-1}$) [40], and was also tested to quench the radicals. In contrast to TBA, the addition of ethanol remarkably inhibited the SCP degradation, with only 44.1% of SCP degraded after 10 min reaction. Since $^{\bullet}OH$ has a minor contribution to SCP degradation, it was possible that other organic radicals could be the major radicals formed in the ZIF-67 activated PAA system [9,14,16]. It was generally acknowledged that $CH_3C(O)OO^{\bullet}$ and $CH_3C(O)O^{\bullet}$ were generated in the $Co^{2+}$ activated PAA system through $Co^{2+}/Co^{3+}$ redox cycling (Eqs. 2 and 3) [12,14]. The active center of ZIF-67 for PAA activation is the 2-methylimidazole coordinated $Co^{2+}$, thus it is reasonable to propose that $CH_3C(O)OO^{\bullet}$ and $CH_3C(O)O^{\bullet}$ could be the dominant radicals in ZIF-67 activated PAA system and contribute to SCP degradation. However, PAA activation

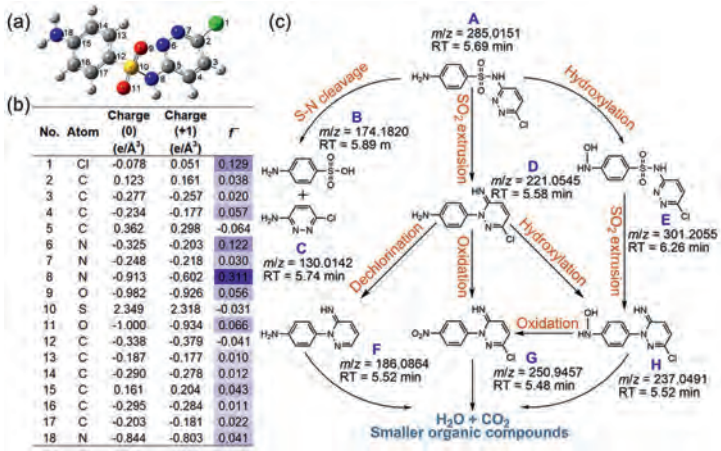


**Fig. 5.** DFT calculation for SCP molecule and degradation intermediates of SCP. (a) Optimized geometry structure of SCP; (b) Fukui index based on DFT calculation at B3LYP/6–31 + G(d, p) level; (c) proposed degradation pathway of SCP based on Fukui index and intermediates detection.

by cobalt is a relatively complex system, and subsequent chain-reaction and self-decay reaction could also occur through Eqs. 4–6. $CH_3C(O)O^{\bullet}$ can attack parent PAA to produce $CH_3C(O)OO^{\bullet}$ (Eq. 4) with a rate constant of $k_{CH_3C(O)O^{\bullet}/PAA} = 0.01–1 \times 10^7$ L mol$^{-1}$ s$^{-1}$, while $CH_3C(O)O^{\bullet}$ can also self-decay to produce $^{\bullet}CH_3$ radical and $CO_2$ (Eq. 5, $k = 1–2.3 \times 10^5$ s$^{-1}$) [10,14]. With the initial concentration of PAA at 50 μmol/L, the reaction rate between $CH_3C(O)O^{\bullet}$ and PAA is around $10^2$ s$^{-1}$, which is three-magnitude slower than the self-decay rate of $CH_3C(O)O^{\bullet}$. Also, $CH_3C(O)O^{\bullet}$ may react with itself through Eq. 6 to form $(CH_3C(O)O)_2$ [14]. Therefore, $CH_3C(O)O^{\bullet}$ is prone to be self-decomposed or self-combined and is not likely to be the dominant radical. Based on the abovementioned discussion, $CH_3C(O)OO^{\bullet}$ with strong oxidation ability is proposed to be the dominant radical rather than $^{\bullet}OH$ and $CH_3C(O)O^{\bullet}$ in ZIF-67 activated PAA system for SCP degradation.

$$CH_3C(O)OOH + Co^{2+} \rightarrow CH_3C(O)O^{\bullet} + Co^{3+} + OH^- \quad (2)$$

$$CH_3C(O)OOH + Co^{3+} \rightarrow CH_3C(O)OO^{\bullet} + Co^{2+} + H^+ \quad (3)$$

$$CH_3C(O)OOH + CH_3C(O)O^{\bullet} \rightarrow CH_3C(O)OO^{\bullet} + CH_3C(O)OH \quad (4)$$

$$CH_3C(O)O^{\bullet} \rightarrow {}^{\bullet}CH_3 + CO_2 \quad (5)$$

$$CH_3C(O)O^{\bullet} + CH_3C(O)O^{\bullet} \rightarrow (CH_3C(O)O)_2 \quad (6)$$

EPR was conducted to directly analyze the ROSs formation. DMPO was used as a trapping agent in this study, which can effectively trap $^{\bullet}OH$, $SO_4^{\bullet-}$, and $O_2^{\bullet-}$ and form a stable complex to facilitate the capture of radical signals [1,35,41], while the specific PAA related organic radicals and DMPO adduct was not clear. In the presence of DMPO and PAA, no signal was captured by DMPO (Fig. 4b), indicating PAA alone could not produce any radical at room temperature and could not oxidize DMPO. Next, after adding ZIF-67 into the DMPO and PAA mixture, a signal of 5,5-dimethyl-2-pyrrolidone-*N*-oxyl (DMPOX, an oxidized form of DMPO) was recorded [18,35]. Unfortunately, no signal of PAA related organic radicals and DMPO adduct was observed. However, the appearance of DMPOX was attributed to the oxidation of DMPO by organic radicals such as $CH_3C(O)OO^{\bullet}$ and $CH_3C(O)O^{\bullet}$ in the ZIF-67 activated PAA system [9,18]. Moreover, the typical DMPO-$^{\bullet}OH$ adduct with the four-line spectrum intensity of 1:2:2:1 was not detected [42,43], which was consistent with the radical quenching experiment results that $^{\bullet}OH$ played a negligible role in the SCP degradation. Taken together, $CH_3C(O)OO^{\bullet}$ is proposed to be the dominant radical in the ZIF-67 activated PAA system rather $CH_3C(O)O^{\bullet}$ and $^{\bullet}OH$.

Afterward, degradation intermediates and Fukui index based on DFT calculation were then studied to elucidate the underlying mechanism of SCP degradation in the ZIF-67 activation PAA system (Fig. 5). Fig. 5a gives the optimized geometry structure of SCP based on DFT and the cartesian coordinates were given in Table S3. $CH_3C(O)OO^{\bullet}$ was identified to be the major radical for SCP degradation, which was considered as electrophile that tends to attack the electron-rich region [16,44]. It is worth noting that $CH_3C(O)OO^{\bullet}$ attack is similar to $SO_4^{\bullet-}$ attack, in which the radical-addition intermediates are hardly detected [8,9]. The Fukui index ($f^-$) for each atom that represents the probability of electrophilic reaction was tabulated in Fig. 5b, *i.e.*, the atom with a higher $f^-$ value is more likely to be attacked by $CH_3C(O)OO^{\bullet}$. Specifically, N8 of SCP with the highest $f^-$ value ($f^- = 0.311$) was the most susceptible site for electrophilic reaction, resulting in the S-N bond cleavage and the formation of intermediates (IMs) B and C (Fig. 5c), which was commonly reported in the previous researches of sulfonamides degradation [45–47]. In addition, $CH_3C(O)OO^{\bullet}$ may also attack N8 by single-electron transfer and form an SCP cationic radical on N8, which was subsequently subjected to a Smile-type rearrangement and the extrusion of $SO_2$ and resulted in the formation of IMs D [24,47,48]. IMs D could be further oxidized to form IMs G (oxidation of amino-group) [11,47], or go through dechlorination and form IMs F. Next, Cl-1 ($f^- = 0.129$), C4 ($f^- = 0.057$), N6 ($f^- = 0.122$), O9 ($f^- = 0.056$), O11 ($f^- = 0.066$), C15 ($f^- = 0.043$), and N18 ($f^- = 0.041$) with relatively high $f^-$ value were discussed. O9 and O11 were first ruled out due to the strong bond energy of O=S=O, while C4 and N6 were also not likely to be attacked by $CH_3C(O)OO^{\bullet}$ owing to the steric hindrance and the high stability of the six-membered heterocyclic ring [47]. C4 also was not a possible site since it was saturated. Therefore, Cl-1 and N18 were preferred sites for $CH_3C(O)OO^{\bullet}$ attack. Electrophilic attack on Cl-1 of SCP may cause the dechlorination or dechlorination/hydroxylation from SCP [49,50]. Unfortunately, no related products were detected, which may be due to the low abundance of these IMs. Attacking N18 by $CH_3C(O)OO^{\bullet}$ can produce SCP cationic radical on N18, which then captured one water molecule with the loss of a proton and formed IMs E [1,51]. IMs E may further go through $SO_2$ extrusion (IMs H) and oxidation to IMs G [24,25]. Finally, with the prolonged reaction time, all the IMs would be further oxidized to smaller organic compounds and ultimately reached $H_2O$ and $CO_2$.

In this study, activation of PAA using MOFs material (ZIF-67) has been first time put forward and tested. ZIF-67 was synthesized *via* a facile direct-mixing method at room temperature, which showed uniform morphology and good crystallinity. ZIF-67 exhibited superior performance for PAA activation and SCP degradation, with 100% of 10 μmol/L SCP degraded within 3 min under optimized conditions. The fitted *pseudo*-first-order rate constant of the ZIF-67 activated PAA system was 34.2 and 156.5 times higher than those of $Co_3O_4$ activated PAA and direct oxidation by PAA. Radical quenching experiments and EPR analysis proposed that $CH_3C(O)OO^{\bullet}$ was the dominant radical rather than $CH_3C(O)O^{\bullet}$ and $^{\bullet}OH$ radicals in ZIF-67 activated PAA system for SCP degradation. Then, the Fukui index based on DFT calculation was used to predict the possible reaction sites of SCP, indicating N8 and N18 were the more preferential sites for electrophilic attack by $CH_3C(O)OO^{\bullet}$. Based on the calculated Fukui index values and intermediates detection, the possible degradation pathway of SCP was proposed, which mainly included the S-N bond cleavage and $SO_2$ extrusion and followed by further oxidation, dechlorination, and hydroxylation. In conclusion, ZIF-67 activated PAA seems a promising approach and holds strong potential for the removal of emerging organic contaminants from water.

## Declaration of competing interest

The authors declare that they have no known competing financial interests or personal relationships that could have appeared to influence the work reported in this paper.

## Acknowledgments

This work is financially supported by the National Natural Science Foundation of China (Nos. 21906001 and 52100069), the National Key Research and Development Program of China (No. 2021YFA1202500), Beijing Nova Program (No. Z191100001119054), and the Fundamental Research Funds for the Central Universities (No. BFUKF202118), and China Postdoctoral Science Foundation (No. 2021M690208).

## Supplementary materials

Supplementary material associated with this article can be found, in the online version, at doi:10.1016/j.cclet.2021.11.072.

## References

[1] J. Ma, L. Chen, Y. Liu, T. Xu, et al., J. Hazard. Mater. 418 (2021) 126180.
[2] W. Yao, S.W. Ur Rehman, H. Wang, et al., Water Res. 138 (2018) 106–117.
[3] D.B. Miklos, R. Hartl, P. Michel, et al., Water Res. 136 (2018) 169–179.
[4] F. Li, J. Duan, S. Tian, et al., Chem. Eng. J. 380 (2020) 122506.
[5] J. Qi, J. Liu, F. Sun, et al., Chin. Chem. Lett. 32 (2021) 1814–1818.
[6] J. Lee, U. Von Gunten, J.H. Kim, et al., Environ. Sci. Technol. 54 (2020) 3064–3081.
[7] M. Li, W. Li, J.R. Bolton, et al., Environ. Sci. Technol. 53 (2019) 912–918.
[8] Y. Shang, X. Xu, B. Gao, et al., Chem. Soc. Rev. 50 (2021) 5281–5322.
[9] Z. Wang, J. Wang, B. Xiong, et al., Environ. Sci. Technol. 54 (2019) 464–475.
[10] J. Kim, T. Zhang, W. Liu, et al., Environ. Sci. Technol. 53 (2019) 13312–13322.
[11] J. Wang, Y. Wan, J. Ding, et al., Environ. Sci. Technol. 54 (2020) 14635–14645.
[12] X. Ao, J. Eloranta, C.H. Huang, et al., Water Res. 188 (2021) 116479.
[13] X. Ao, W. Wang, W. Sun, et al., Water Res. 203 (2021) 117458.
[14] J. Kim, P. Du, W. Liu, et al., Environ. Sci. Technol. 54 (2020) 5268–5278.
[15] R. Li, K. Manoli, J. Kim, et al., Environ. Sci. Technol. 55 (2021) 9150–9160.
[16] B. Liu, W. Guo, W. Jia, et al., Water Res. 201 (2021) 117313.
[17] J. Lin, Y. Hu, J. Xiao, et al., Chem. Eng. J. 420 (2021) 129692.
[18] W. Wu, D. Tian, T. Liu, et al., Chem. Eng. J. 394 (2020) 124938.
[19] X. Du, M. Zhou, Chem. Eng. J. 403 (2021) 126346.
[20] C. Wang, J. Kim, V. Malgras, et al., Small 15 (2019) 1900744.
[21] Y. Shang, X. Duan, S. Wang, et al., Chin. Chem. Lett. 33 (2022) 663–673.
[22] Q. Yang, S.S. Ren, Q. Zhao, et al., Chem. Eng. J. 333 (2018) 49–57.
[23] Y. Ji, Y. Shi, L. Wang, et al., Sci. Total Environ. 593–594 (2017) 704–712.
[24] X. Sun, M. Feng, S. Dong, et al., Chem. Eng. J. 372 (2019) 742–751.
[25] X. Tao, P. Pan, T. Huang, et al., Chem. Eng. J. 395 (2020) 125186.
[26] R. Li, R. Che, Q. Liu, et al., J. Hazard. Mater. 338 (2017) 167–176.
[27] J. Qin, S. Wang, X. Wang, Appl. Catal. B: Environ. 209 (2017) 476–482.
[28] J. Wang, Z. Wang, Y. Cheng, et al., Water Res. 201 (2021) 117291.
[29] M.J. Frisch, G.W. Trucks, H.B. Schlegel, et al., Gaussian 16, Revision C.01, Gaussian, Inc., Wallingford CT, (2016).
[30] X. Guo, T. Xing, Y. Lou, et al., J. Solid State Chem. 235 (2016) 107–112.
[31] X.D. Du, C.C. Wang, J.G. Liu, et al., J. Colloid Interface Sci. 506 (2017) 437–441.
[32] W. Zhang, X. Jiang, X. Wang, et al., Angew. Chem. Int. Ed. 56 (2017) 8435–8440.
[33] D. He, X. Song, W. Li, et al., Angew. Chem. 132 (2020) 6996–7002.
[34] H. Zhou, M. Zheng, H. Tang, et al., Small 16 (2020) 1904252.
[35] L. Chen, H. Ji, J. Qi, et al., Chem. Eng. J. 406 (2021) 126877.
[36] M. Wang, J. Liu, C. Guo, et al., J. Mater. Chem. A 6 (2018) 4768–4775.
[37] J. Duan, H. Ji, T. Xu, et al., Chem. Eng. J. 406 (2021) 126752.
[38] J. Duan, H. Ji, X. Zhao, et al., Chem. Eng. J. 393 (2020) 124692.
[39] M.R. Azhar, H.R. Abid, V. Periasamy, et al., J. Colloid Interface Sci. 500 (2017) 88–95.
[40] C. Zhu, F. Zhu, D.D. Dionysiou, et al., Water Res. 139 (2018) 66–73.
[41] C. Hwang, J.T. Yoo, G.Y. Jung, et al., ACS Nano 13 (2019) 9190–9197.
[42] S. Yanan, X. Xing, Q. Yue, et al., Environ. Sci. Nano 7 (2020) 1444–1453.
[43] P. Duan, Y. Qi, S. Feng, et al., Appl. Catal. B: Environ. 267 (2020) 118717.
[44] M. Hoshino, M. Kagata, H. Seki, et al., J. Am. Chem. Soc. 118 (1996) 2160–2165.
[45] Y. Liu, L. Chen, X. Liu, et al., Chin. Chem. Lett. 33 (2022) 1385–1389.
[46] H. Ji, P. Du, D. Zhao, et al., Appl. Catal. B: Environ. 263 (2020) 118357.
[47] J. Li, L. Zhao, M. Feng, et al., Water Res. 202 (2021) 117463.
[48] J. Gao, C. Hedman, C. Liu, et al., Environ. Sci. Technol. 46 (2012) 2642–2651.
[49] X. Li, X. Liu, C. Lin, et al., Chem. Eng. J. 367 (2019) 208–218.
[50] A. Dirany, I. Sirés, N. Oturan, et al., Environ. Sci. Technol. 46 (2012) 4074–4082.
[51] G.X. Huang, J.Y. Si, C. Qian, et al., Anal. Chem. 90 (2018) 14439–14446.